The type Ia supernova SNLS-03D3bb from a super-Chandrasekhar-mass white dwarf star

D.A. Howell, M. Sullivan, P.E. Nugent, R.S. Ellis, A.J. Conley, Damien Le Borgne, R.G. Carlberg, J. Guy, D. Balam, S. Basa, et al.

The type Ia supernova SNLS-03D3bb from a super-Chandrasekhar-mass white dwarf star

D. Andrew Howell[1], Mark Sullivan[1], Peter E. Nugent[2], Richard S. Ellis[3], Alexander J. Conley[1], Damien Le Borgne[4], Raymond G. Carlberg[1], Julien Guy[5], David Balam[6], Stephane Basa[7], Dominique Fouchez[8], Isobel M. Hook[9], Eric Y. Hsiao[6], James D. Neill[6], Reynald Pain[5], Kathryn M. Perrett[1], Christopher J. Pritchet[6]

[1]*Department of Astronomy and Astrophysics, University of Toronto, 60 St. George Street, Toronto, ON M5S 3H8, Canada*
[2]*Lawrence Berkeley National Laboratory, Mail Stop 50-232, 1 Cyclotron Road, Berkeley CA 94720 USA*
[3]*California Institute of Technology, E. California Blvd., Pasadena, CA 91125, USA*
[4]*DAPNIA/Service d'Astrophysique, CEA/Saclay, 91191 Gif-sur-Yvette Cedex, France*
[5]*LPNHE, CNRS-IN2P3 and University of Paris VI & VII, 75005 Paris, France*
[6]*Department of Physics and Astronomy, University of Victoria, PO Box 3055, Victoria, BC V8W 3P6, Canada*
[7]*LAM CNRS, BP8, Traverse du Siphon, 13376 Marseille Cedex 12, France*
[8]*CPPM, CNRS-IN2P3 and University Aix Marseille II, Case 907, 13288 Marseille Cedex 9, France*
[9]*University of Oxford Astrophysics, Denys Wilkinson Building, Keble Road, Oxford OX1 3RH, UK*

The acceleration of the expansion of the universe, and the need for Dark Energy, were inferred from the observations of Type Ia supernovae (SNe Ia)[1;2]. There is consensus that SNe Ia are thermonuclear explosions that destroy carbon-oxygen white dwarf stars that accrete matter from a companion star[3], although the nature of this companion remains uncertain. SNe Ia are thought to be reliable distance indicators because they have a standard amount of fuel and a uniform trigger — they are predicted to explode when the mass of the white dwarf nears the Chandrasekhar mass[4] — 1.4 solar masses. Here we show that the high redshift supernova SNLS-03D3bb has an exceptionally high luminosity and low kinetic energy that both imply a *super*-Chandrasekhar mass progenitor. Super-Chandrasekhar mass SNe Ia should preferentially occur in a young stellar population, so this may provide an explanation for the observed trend that overluminous SNe Ia only occur in young environments[5;6]. Since this supernova does not obey the relations that allow them to be calibrated as standard candles, and since no counterparts have been found at low redshift, future cosmology studies will have to consider contamination from such events.

SNLS-03D3bb (SN 2003fg) was discovered on April 24, 2003 (UT) as part of the Supernova Legacy Survey (SNLS). Its redshift is $z = 0.2440 \pm 0.0003$, determined from host galaxy [OII], [OIII], Hα, and Hβ emission lines. A finding chart and observational details can be found in the supplementary information (SI). From the lightcurve (Figure 1) we measure a peak magnitude in the rest frame V band, $V = 20.50 \pm 0.06$ mag. This corresponds to an absolute magnitude of $M_V = -19.94 \pm 0.06$ ($H_0 = 70$ km s^{-1} Mpc^{-1}, $\Omega_M = 0.3$, flat universe). SNLS-03D3bb falls completely outside of the M_V distribution of low-z SNe Ia[7], and is 0.87 mag (a factor of 2.2) brighter than the median. Note that neither changes in the Hubble constant nor Ω_M significantly affect this brightness difference. Asphericity may account for variations in SN Ia luminosity at the 25% level, but not a factor of two[8;9]. SNLS-03D3bb also does not follow the lightcurve width-luminosity relationship[10] for SNe Ia that allows them to be calibrated as standard candles — it is too bright for its lightcurve width ("stretch", s=1.13) by 0.61 ± 0.14 mag (4.4σ).

Type Ia supernovae are powered exclusively by the decay of $^{56}\mathrm{Ni}$ and its decay product $^{56}\mathrm{Co}$[11], requiring $\sim 0.6\ \mathrm{M}_\odot$ of $^{56}\mathrm{Ni}$ to reproduce a normal SNe Ia[12;13;14;15]. Since SNLS-03D3bb is 2.2 times overluminous, this implies that it has $\sim 1.3\ \mathrm{M}_\odot$of $^{56}\mathrm{Ni}$. Such a large $^{56}\mathrm{Ni}$ mass is not possible if the progenitor is limited to the Chandrasekhar mass (1.4 $\mathrm{M}_\odot$). Even models that burn the entire 1.4 $\mathrm{M}_\odot$ to nuclear statistical equilibrium via a pure detonation produce only 0.92 $\mathrm{M}_\odot$ of $^{56}\mathrm{Ni}$, with the remainder comprising other iron-peak elements[16]. Since at least 40% of the SN Ia must be elements other than $^{56}\mathrm{Ni}$ to reproduce observed spectra[14;17], this implies a WD mass of $\sim 2.1\ \mathrm{M}_\odot$. Some authors find rapid rotation may support such a massive white dwarf[18]. The merger of two massive white dwarfs could also produce a super-Chandrasekhar product[19;20].

This simple estimation of the nickel mass is supported by a more detailed calculation using the principle that the luminosity at maximum light is proportional to the instantaneous rate of radioactive decay[21;22]. The impied Ni mass is[23;24]: $M_{\mathrm{Ni}} = \frac{L_{\mathrm{bol}}}{\alpha \dot{S}(t_R)}$, where L_{bol} is the bolometric luminosity at maximum light (the luminosity integrated from the ultraviolet to the infrared), and α is the ratio of bolometric to radioactivity luminosities, near unity. $\dot{S}$ is the radioactivity luminosity per solar mass of $^{56}\mathrm{Ni}$ from its decay to $^{56}\mathrm{Co}$ and subsequent decay to $^{56}\mathrm{Fe}$: $\dot{S} = 6.31 \times 10^{43} e^{-t_R/8.8} + 1.43 \times 10^{43} e^{-t_R/111}\ \mathrm{erg\ s^{-1}\ M_\odot^{-1}}$, where t_R is the time in days for the supernova to rise from explosion to maximum light. Using $t_R = s \times 19.5$ days[25], for SNLS-03D3bb, $t_R = 22$ days (see SI for the effect of a shorter rise). We use $\alpha = 1.2$ as a conservative value, although for high $^{56}\mathrm{Ni}$ masses, α may be lower, since nickel above the photosphere will not contribute to the luminosity[23].

To convert our V magnitude into a bolometric equivalent, we use a synthetic spectrum calculated to match the observed UV+optical spectrum (Fig. 3), but extended into the infrared (13% of the bolometric luminosity is from the IR extrapolation). The bolometric correction (m_{bc}) is 0.07 ± 0.03 mag, such that $M_{\mathrm{bol}} = M_V + m_{\mathrm{bc}} = -19.87 \pm 0.06$ mag. Using these numbers, we calculate $M_{\mathrm{Ni}} = 1.29 \pm 0.07\ \mathrm{M}_\odot$ for SNLS-03D3bb, in agreement with the simple scaling argument used earlier. The quoted error is from the statistical, k-correction, and bolometric correction errors added in quadrature. SNLS-03D3bb has a significantly larger bolometric luminosity and implied $^{56}\mathrm{Ni}$ mass compared to low redshift SNe (Fig. 2).

SNLS-03D3bb also has an unusually low ejecta velocity, as shown in the Keck spetrum taken 2 days after maximum light (Fig. 3). With a SiII velocity of 8000 ± 500 km s^{-1}, it falls well outside the range of velocities seen for this feature at maximum light (Fig. 4). This is hard to understand in the Chandrasekhar mass model, which predicts *higher* velocities for more luminous SNe Ia, in contrast to the unusually *low* velocities in SNLS-03D3bb.

The kinetic energy (E_k) of a SN Ia arises from the difference between the nuclear energy (E_n) obtained from the synthesis of elements via fusion in the explosion and the binding energy

(E_b) of the white dwarf[13]. Thus the kinetic energy velocity is: $v_{\rm ke} = \sqrt{\frac{2(E_n - E_b)}{M_{\rm WD}}}$, where $M_{\rm WD}$ is the mass of the white dwarf. The binding energy of a 1.4 $\mathrm{M}_\odot$ C/O WD is 0.5×10^{51} ergs[14]. For a $2\mathrm{M}_\odot$ WD and a central density of 4×10^9 g cm^{-3}, the binding energy is 1.3×10^{51} ergs[18].

Since there are only three classes of elements in a SN Ia (iron-peak elements, intermediate mass elements (IME), and unburned carbon and oxygen), a simple model can be developed for the nuclear energy generation, E_n. Burning a mixture of equal parts carbon and oxygen to the iron peak produces $E_{\rm Fe} = 1.55 \times 10^{51}$ erg $\mathrm{M}_\odot{}^{-1}$, while the synthesis of ^{28}Si produces 76% as much energy[13]. Thus: $E_n = E_{\rm Fe} M_{\rm WD}(f_{\rm Fe} + 0.76 f_{\rm IME})$, where $M_{\rm WD}$ is in solar masses, and $f_{\rm Fe}$ and $f_{\rm IME}$ are the fractional compositions of iron peak and intermediate mass elements. If $f_{\rm Fe}$ and $f_{\rm IME}$ do not sum to one, the remainder is the fraction of unburned carbon and oxygen (f_C), which does not contribute to the nuclear energy. The $^{56}\mathrm{Ni}$ makes up approximately 70% of iron-peak elements[14;16], so we adopt $M_{\rm Ni} = 0.7 M_{\rm WD} f_{\rm Fe}$, where $M_{\rm Ni}$ is the mass of $^{56}\mathrm{Ni}$.

In the Chandrasekhar mass model, more luminous SNe, with more $^{56}\mathrm{Ni}$, have a higher $v_{\rm ke}$ (Fig. 4). Increasing the fraction of unburned carbon and oxygen, f_C, can lower the kinetic energy, perhaps accounting for some of the dispersion in SN Ia velocities. However, this also lowers the available $^{56}\mathrm{Ni}$, so it cannot account for the low velocity seen in SNLS-03D3bb.

The kinetic energy gives the velocity of the supernova averaged over the entire mass, approximately equivalent to the velocity a few weeks after maximum light[13]. The most appropriate observational signature of this velocity is unclear, since SN Ia line velocities change with time, and different ions can have different relative velocities. We find good agreement between the SiII velocity at 40 days after maximum light[26] and the theoretical kinetic energy velocity, but we emphasize that this is in imperfect comparison.

A super-Chandrasekhar mass reproduces the low velocities seen in SNLS-03D3bb (Fig. 4). Since Chandrasekhar models with more Ni produce higher velocities, the low velocities of SNLS-03D3bb imply an increased progenitor binding energy and thus a larger total mass. As a caveat, we note that this simple calculation is only intended to illustrate general trends. Future theoretical studies will have to assess such complications as using different ions, different white dwarf density structures, and a wider range of binding energies.

Super-Chandrasekhar mass SNe Ia should be more likely in a young stellar population, where the most massive stars exist[19;20]. The low mass, star forming host of SNLS-03D3bb is consistent with this scenario (see SI). Thus, the apparent existence of super-Chandrasekhar mass SNe Ia may explain why the most luminous SNe Ia only occur in young stellar environments[5;6]. The standard Chandrasekhar mass model offers no explanation for this behaviour, since the total amount of fuel and triggering mechanism should be independent of the mass of the progenitor stars.

SNe such as SNLS-03D3bb will have to be screened out in cosmological studies. Since younger stellar environments produce more luminous SNe, as the mean stellar age decreases with redshift the mean properties of SNe Ia will change[5]. This can be calibrated if all SNe obey the same stretch-luminosity relationship, but SNLS-03D3bb does not. Its peculiarity was so obvious that it was excluded from the SNLS cosmological result[7], but less extreme objects could lurk in SN samples. Future cosmology studies will have to carefully scrutinise SNe Ia from young populations to see if they obey the same lightcurve shape-luminosity relationship as other SNe Ia.

1. Perlmutter, S. *et al.* Measurements of Omega and Lambda from 42 High-Redshift Supernovae. *Astrophys. J.* **517**, 565–586 (1999).

2. Riess, A. G. *et al.* Observational Evidence from Supernovae for an Accelerating Universe and a Cosmological Constant. *Astron. J.* **116**, 1009–1038 (1998).

3. Hoyle, F. & Fowler, W. A. Nucleosynthesis in Supernovae. *Astrophys. J.* **132**, 565–590 (1960).

4. Chandrasekhar, S. The Maximum Mass of Ideal White Dwarfs. *Astrophys. J.* **74**, 81–82 (1931).

5. Sullivan, M. *et al.* Rates and properties of type Ia supernovae as a function of mass and star-formation in their host galaxies. *Astrophys. J., in press* (2006). `astro-ph/0605455`.

6. Hamuy, M. *et al.* The Absolute Luminosities of the Calan/Tololo Type IA Supernovae. *Astron. J.* **112**, 2391–2397 (1996).

7. Astier, P. *et al.* The Supernova Legacy Survey: measurement of Ω_M, Ω_Λ and w from the first year data set. *Astron. & Astrophys.* **447**, 31–48 (2006).

8. Howell, D. A., Höflich, P., Wang, L. & Wheeler, J. C. Evidence for Asphericity in a Subluminous Type Ia Supernova: Spectropolarimetry of SN 1999by. *Astrophys. J.* **556**, 302–321 (2001).

9. Kasen, D., Nugent, P., Thomas, R. C. & Wang, L. Could There Be a Hole in Type Ia Supernovae? *Astrophys. J.* **610**, 876–887 (2004).

10. Phillips, M. M. The absolute magnitudes of Type IA supernovae. *Astrophys. J. Lett.* **413**, L105–L108 (1993).

11. Colgate, S. A. & McKee, C. Early Supernova Luminosity. *Astrophys. J.* **157**, 623–644 (1969).

12. Woosley, S. E. & Weaver, T. A. The physics of supernova explosions. *Ann. Rev. Astron. Astrophys.* **24**, 205–253 (1986).

13. Branch, D. The Hubble constant from nickel radioactivity in type IA supernovae. *Astrophys. J.* **392**, 35–40 (1992).

14. Nomoto, K., Thielemann, F.-K. & Yokoi, K. Accreting white dwarf models of Type I supernovae. III - Carbon deflagration supernovae. *Astrophys. J.* **286**, 644–658 (1984).

15. Hoflich, P. Analysis of the type IA supernova SN 1994D. *Astrophys. J.* **443**, 89–108 (1995).

16. Khokhlov, A., Mueller, E. & Hoeflich, P. Light curves of Type IA supernova models with different explosion mechanisms. *Astron. & Astrophys.* **270**, 223–248 (1993).

17. Fisher, A., Branch, D., Hatano, K. & Baron, E. On the spectrum and nature of the peculiar Type IA supernova 1991T. *MNRAS* **304**, 67–74 (1999).

18. Yoon, S.-C. & Langer, N. On the evolution of rapidly rotating massive white dwarfs towards supernovae or collapses. *Astron. & Astrophys.* **435**, 967–985 (2005).

19. Tutukov, A. V. & Yungelson, L. R. Merging of Binary White Dwarfs Neutron Stars and Black-Holes Under the Influence of Gravitational Wave Radiation. *MNRAS* **268**, 871–879 (1994).

20. Howell, D. A. The Progenitors of Subluminous Type Ia Supernovae. *Astrophys. J. Lett.* **554**, L193–L196 (2001).

21. Arnett, W. D. Type I supernovae. I - Analytic solutions for the early part of the light curve. *Astrophys. J.* **253**, 785–797 (1982).

22. Arnett, W. D., Branch, D. & Wheeler, J. C. Hubble's constant and exploding carbon-oxygen white dwarf models for Type I supernovae. *Nature* **314**, 337–338 (1985).

23. Nugent, P. *et al.* Low Hubble Constant from the Physics of Type Ia Supernovae. *Physical Review Letters* **75**, 394–397 (1995).

24. Nugent, P. E. Non-Local Thermodynamic Equilibrium Spectrum Synthesis of Type IA Supernovae. *Ph.D. Thesis* (1997).

25. Conley, A. *et al.* The rise time of Type Ia supernovae from the Supernova Legacy Survey. *Astron. J., submitted* (2006).

26. Benetti, S. *et al.* The Diversity of Type Ia Supernovae: Evidence for Systematics? *Astrophys. J.* **623**, 1011–1016 (2005).

27. Nugent, P., Kim, A. & Perlmutter, S. K-Corrections and Extinction Corrections for Type Ia Supernovae. *PASP* **114**, 803–819 (2002).

28. Bessell, M. S. Ubvri passbands. *PASP* **102**, 1181–1199 (1990).

29. Fisher, A., Branch, D., Nugent, P. & Baron, E. Evidence for a High-velocity Carbon-rich Layer in the Type IA SN 1990N. *Astrophys. J. Lett.* **481**, L89–L92 (1997).

30. Marion, G. H. *et al.* Low Carbon Abundance in Type Ia Supernovae. *ArXiv Astrophysics e-prints* (2006). `arXiv:astro-ph/0601614`.

Supplementary Information is linked to the online version of this paper at www.nature.com/nature.

Acknowledgements SNLS relies on observations with MegaCam, a joint project of CFHT and CEA/DAPNIA, at the Canada-France-Hawaii Telescope (CFHT). We used data products produced at the Canadian Astronomy Data Centre as part of the CFHT Legacy Survey. Some data were obtained at the W.M. Keck Observatory. We acknowledge support from NSERC, NERSC, CIAR, CNRS/IN2P3, CNRS/INSU, CEA, and the DOE.

Author Infomation Reprints and permissions information is available at npg.nature.com/reprintsandpermissions. The authors declare no competing financial interests. Correspondence and requests for materials should be addressed to D.A.H (howell@astro.utoronto.ca).

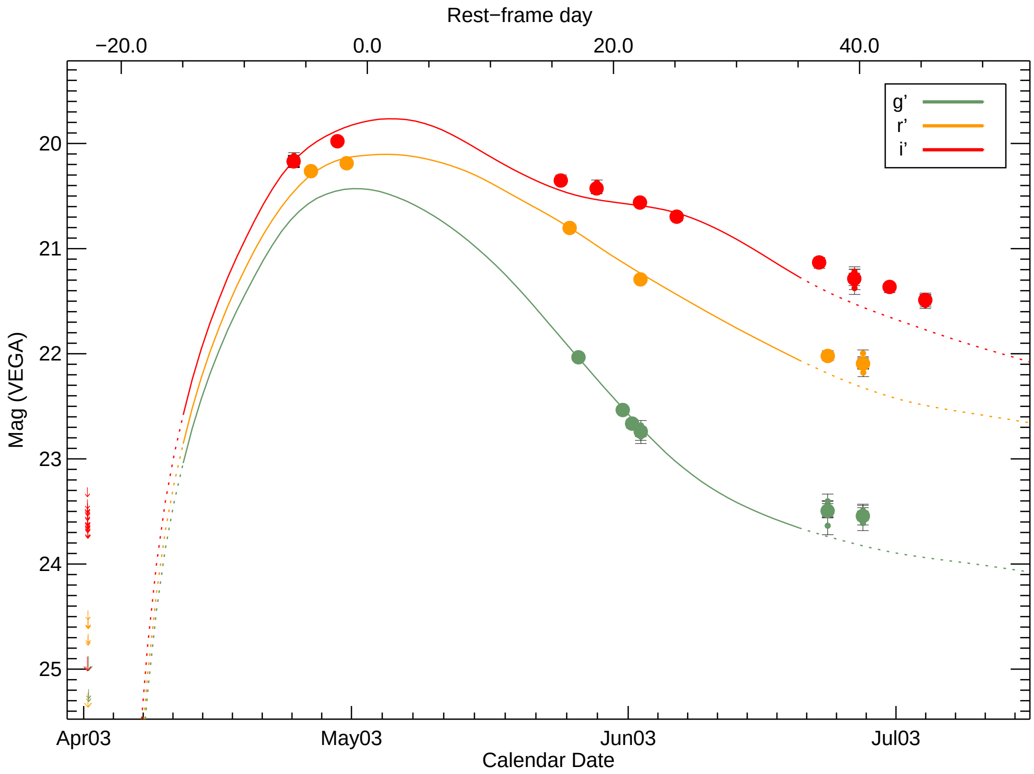

Figure 1: The lightcurve of SNLS-03D3bb. We fit k-corrected[27] template lightcurves to the observed photometry of SNLS-03D3bb, then transform the peak magnitudes back to the Johnson-Cousins[28] BV magnitudes in the Vega system. We find peak magnitudes of $B = 20.35$ mag and $V = 20.50 \pm 0.06$ mag from a simultaneous fit to g' and r' data. The error (s.d.) consists of 0.04 statistical error and 0.04 k-correction error. A lightcurve template was fit using the stretch method[1] (stretching the time axis of a template lightcurve by a stretch factor, $s = 1.13$). The epoch of maximum light relative to the rest frame B band was determined from a simultaneous fit to all of the data. At maximum, we only use the V band value to compare to other SNe, since it is the best constrained. Data past +35 days was not used in the fit. The arrows are three sigma upper limits.

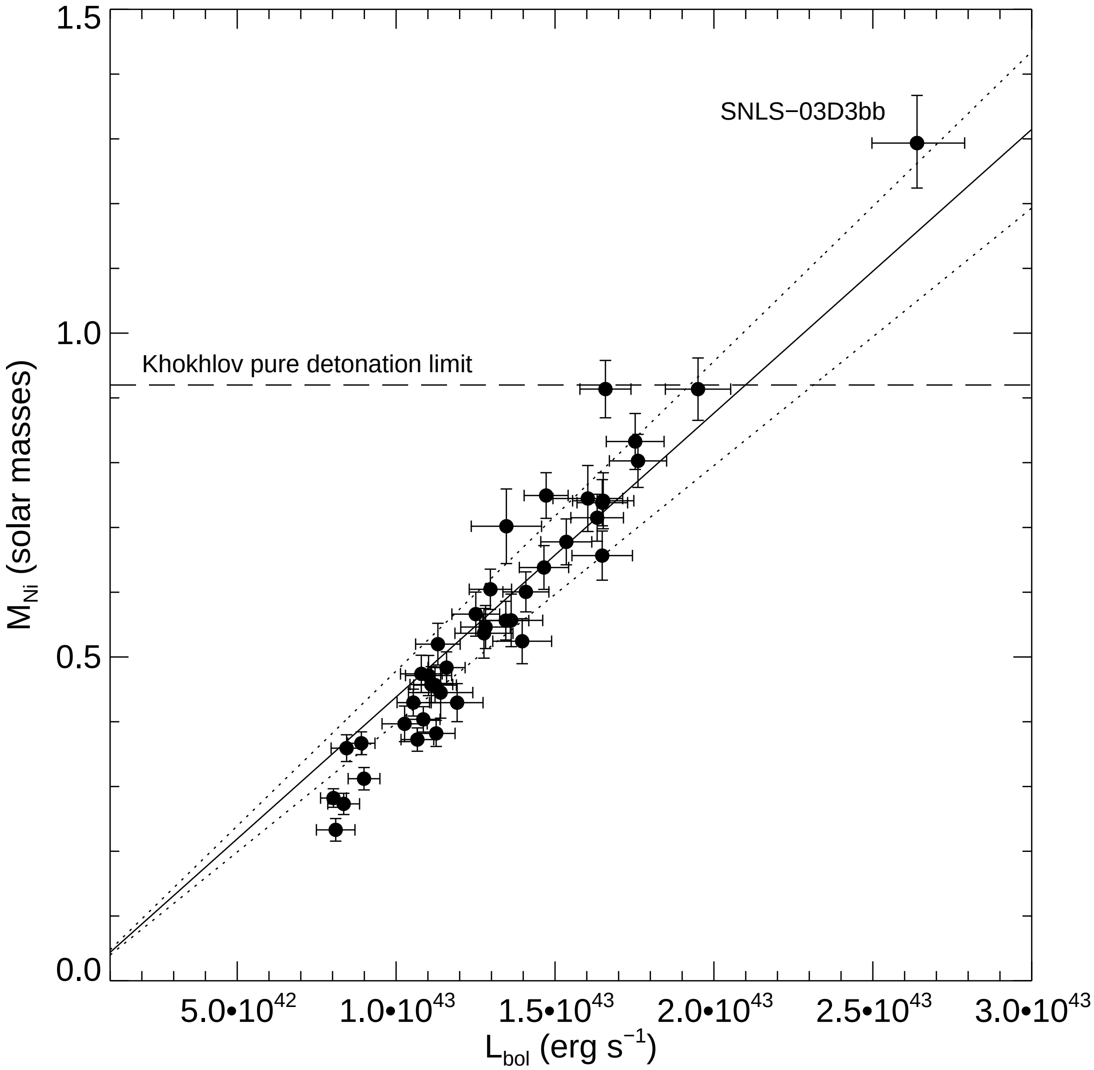

Figure 2: Bolometric luminosity vs. implied ^{56}Ni mass for SNLS-03D3bb and low redshift SNe Ia[7]. The low redshift SNe Ia were fit using the same techniques as those used for SNLS-03D3bb: the bolometric luminosity was determined using the peak magnitude in the V band from a simultaneous fit to B and V band data. For the low redshift SNe Ia, we integrated the s=1 SN template[27] to obtain a bolometric correction of 0.06 magnitudes and an uncertainty (s.d.) of 0.05 mag for the combined bolometric and k-correction error. The solid line represents a normal stretch=1 SN Ia, with a rise time (t_r) of -19.5 days, while dotted lines show $s = 0.9$ ($t_r = 17.6$) and $s = 1.1$ ($t_r = 21.5$). Low luminosity SNe Ia have lower stretches, and thus shorter rise times, resulting in less ^{56}Ni for a given luminosity, while high stretch SNe Ia show opposite behaviour. The dashed line shows an upper limit for the expected ^{56}Ni mass in a Chandrasekhar mass SN Ia, obtained by burning the entire white dwarf to iron-peak elements in a detonation[16].

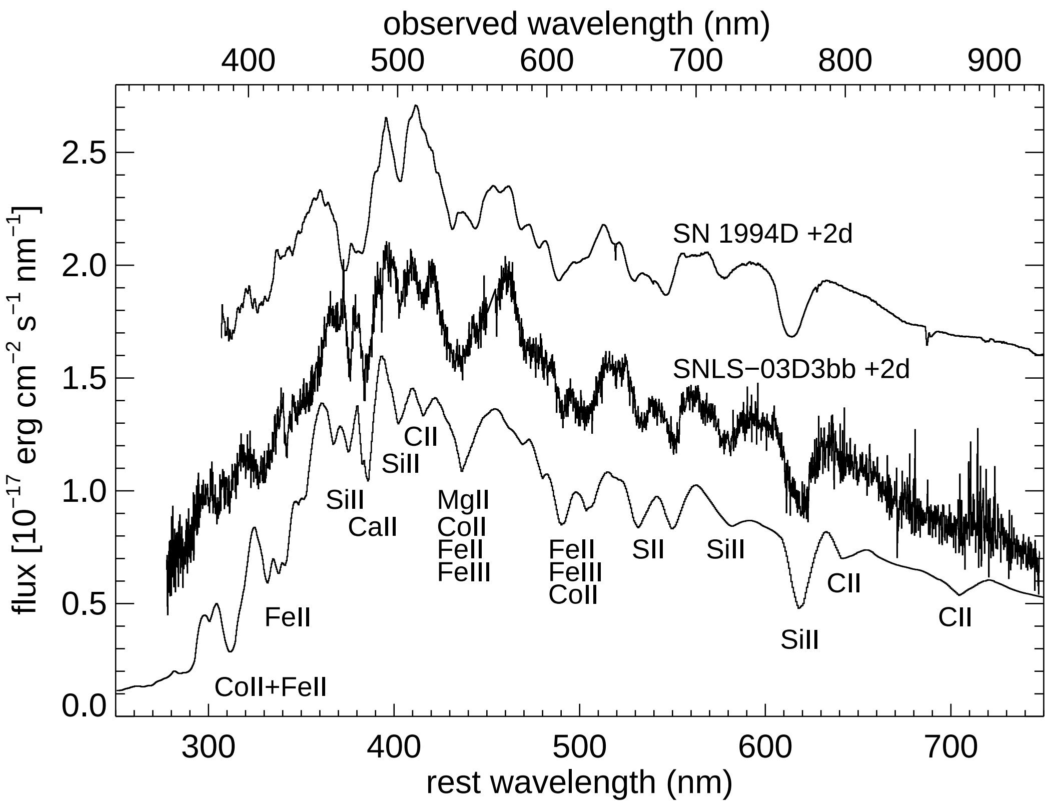

Figure 3: Keck LRIS spectrum of SNLS-03D3bb at 2 days after maximum light compared to a spectrum of the normal Type Ia SN 1994D. Also plotted is a SYNOW fit to the data with dominant ions labeled. SYNOW is a parameterized resonance-scattering code, allowing the user to adjust optical depths, temperatures, and velocities to aid in the identification of supernova lines[29]. SYNOW parameters are listed in the supplementary information. SNLS-03D3bb shows the lines of IMEs typically seen in a SN Ia at maximum light — SiII, SII, and CaII, but in SNLS-03D3bb the velocity of the lines is lower than usual. The line at 415 nm appears to be CII, but the other predicted carbon features cannot be clearly identified due to the lower signal-to-noise ratio of the spectrum in the red. No other identification could be found for the 415 nm feature.

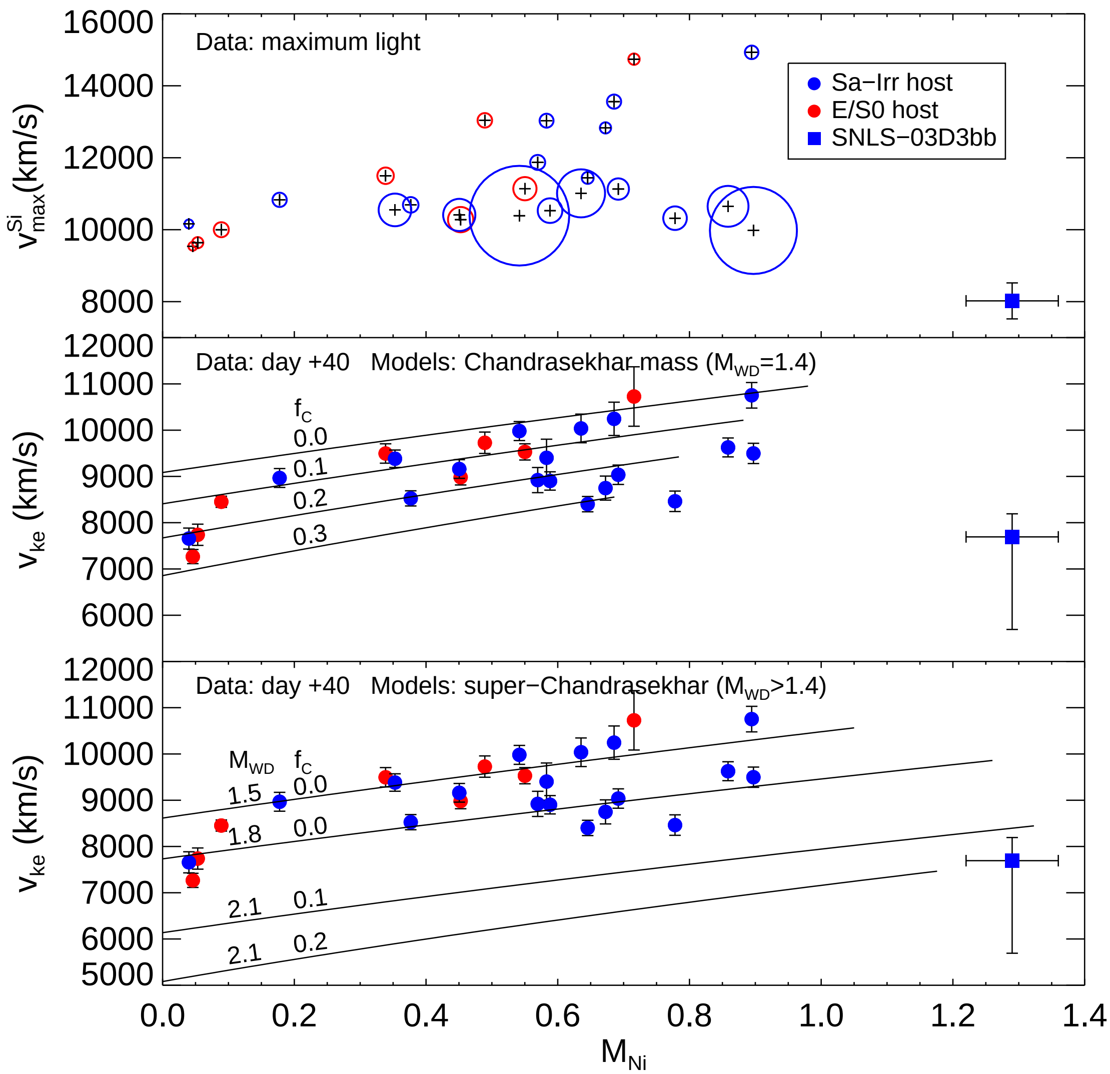

Figure 4: Inferred Ni mass vs. SiII 615 nm velocity. **a**, The data at maximum light[26]. Ni masses are converted as described in the text using $M_{\rm bol} = M_B + 0.2$. Red circles are from early type galaxies (E or S0), while blue circles are from late type galaxies (Sa-Irr). Circle size is proportional to $v_{\rm Si}/\dot{v}_{\rm Si}$, where $\dot{v}_{\rm Si}$ is the rate of change of the velocity of the SiII feature. There is no $\dot{v}_{\rm Si}$ measurement for SNLS-03D3bb. **b**, Kinetic energy velocity of SNe Ia versus Ni mass for 1.4 solar mass models with different fractions of unburned carbon (f_C). This unburned fraction should not be much higher than $\sim 20\%$ because carbon is rarely seen in SN Ia spectra[30]. Overplotted symbols are $v_{\rm Si}$ for low redshift SNe Ia[26] extrapolated to 40 days after maximum (correcting for stretch). For SNLS-03D3bb we use $\dot{v}_{\rm Si}$ from its closest neighbor. The error bar reflects the range if an average value of $\dot{v}_{\rm Si}$ is used. SNLS-03D3bb is not consistent with the 1.4 $\rm M_\odot$ model. **c**, As above, but showing that $M_{\rm WD} \sim 2\ \rm M_\odot$ models can explain SNLS-03D3bb. Less extreme super-Chandrasekhar mass models are consistent with the low redshift data. The three low ^{56}Ni SNe are not necessarily super-Chandrasekhar SNe Ia — their large values of $\dot{v}_{\rm Si}$ make projections to 40 days uncertain.